Donor−Acceptor Interaction in Cationic Archetype Mono- and Dinuclear Sesquifulvalene Complexes $[(\eta^5\text{-}C_5H_5)Fe\{\mu\text{-}(\eta^5\text{-}C_5H_4)(\eta^7\text{-}C_7H_6)\}M'L']^{n+}$ (n = 1, 2)

Timo Meyer-Friedrichsen,[a] Christoph Mecker,[a] Marc H. Prosenc,[a] and Jürgen Heck*[a]

Dedicated to Prof. Dr. Thiem on the occasion of his 60th birthday

Keywords: Nonlinear optics / Sesquifulvalene complexes / Structure determination / Cyclic voltammetry / Iron / Ruthenium

In order to gain a deeper insight into structure-property relationships of the donor (D)–acceptor (A) interactions in cationic sesquifulvalene complexes the mono- and dicationic complexes $[(\eta^5\text{-}C_5H_5)Fe\{\mu\text{-}(\eta^5\text{-}C_5H_4)(\eta^7\text{-}C_7H_6)\}M'L']^+$ were synthesized as BF_4 and PF_6 salts: M′L′ = $Cr(CO)_3$ (**3**PF_6); M′L′ = none (**4**BF_4); M′L′ = $Ru(\eta^5\text{-}C_5H_5)^+$ [**5**$(PF_6)_2$]; M′L′ = $Ru(\eta^5\text{-}C_5Me_5)^+$ [**6**$(PF_6)_2$]. The ferrocenyl substituent works as the electron donor and the tropylium moiety as the electron acceptor. For the electronic ground state the NMR spectroscopic results demonstrate an increasing charge delocalization in the order M′L′ = $Cr(CO)_3$ < $Ru(\eta^5\text{-}C_5Me_5)^+$ < $Ru(\eta^5\text{-}C_5H_5)$ < none. The same order of the acceptor moieties is observed for the difference between the oxidation and reduction potentials, which are related to an electrochemically reversible and a complete irreversible one-electron transfer, respectively. A comparison of the structural data of **3**–**6** reveals a small but distinct contribution of the cross-conjugated mesomeric form to the bis(aromatic) mesomeric form in the ground state of the sesquifulvalene complexes, which increases, when the electron-withdrawing ability of the acceptor becomes stronger. The UV/Vis spectra are dominated by two intense absorption bands in the visible and near-UV region, which are assigned to a low-energy donor-(metal)–acceptor charge-transfer (D–A CT) transition and to a high-energy donor(ligand)–acceptor charge-transfer (L–A CT) transition. For these archetype sesquifulvalene complexes the first hyperpolarizability β was determined by means of hyper-Rayleigh scattering (HRS). Whereas for **3** no second harmonic signal could be detected and **4** shows fluorescence due to two-photon absorptions, **5** and **6** possess appreciable β values.

Introduction

Structure-property relationships in nonlinear optical (NLO) chromophores have proven to be very useful, in particular for organic polyene-bridged donor−acceptor (D−A) molecules, as it has been demonstrated for the bond-length alternation (BLA) in relation to second harmonic generation (SHG).[1,2] As in D−A substituted polyenes, a description of the bonding situation in mono- and dinuclear sesquifulvalene complexes which demonstrates weak to strong NLO effects, is achieved by different mesomeric forms. The ground state is mainly represented by the polar bisaromatic form **A** as deduced by means of several structure determinations, whereas the excited CT state is supposed to have more contributions from the cross-conjugated form **B** (Figure 1).[3,4]

It would be worthwhile to know, whether a contribution of the cross-conjugated form **B** to the ground state would affect the SHG according to the BLA in acyclic α,ω-donor−acceptor substituted conjugated polyenes.

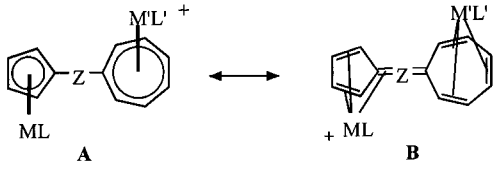

Figure 1. The bis(aromatic) (**A**) and cross-conjugated (**B**) form of mono- and dinuclear sesquifulvalene complexes [e.g. ML = $Fe(\eta^5\text{-}C_5H_5)$; M′L′ = none, $Cr(CO)_3$; Z denotes a conjugated π-bridge]

The crystal structure determinations of the hitherto structurally characterized mono- and dinuclear sesquifulvalene-type complexes do not indicate any significant contribution of the cross-conjugated form **B** to the ground state. This is partly due to the poor quality of the crystals, resulting in a low accuracy of the crystal structure analyses, and partly due to the fact that there are no structural changes, which point to the lack of any remarkable delocalization of charge.[3−7] However, we were now able to determine the structures of some sesquifulvalene complexes, wherein the five- and seven-membered rings are directly connected, in sufficiently high quality to discuss some structure−property relationships. In this paper we additionally present syntheses, spectroscopic and redox properties of the mono- and dinuclear archetype

[a] Institut für Anorganische und Angewandte Chemie
Martin-Luther-King-Platz 6, 20146 Hamburg, Germany
Fax: (internat.) + 49-(0)40/42838-6945
E-mail: heck@chemie.uni-hamburg.de

  1434−1948/02/0101−0239 $ 17.50+.50/0

sesquifulvalene complexes depicted in Figure 2, as well as results of NLO studies concerning the SHG. The spectroscopic and redox data are discussed in comparison to the corresponding properties of the tropylium cation and its complexes shown in Figure 2.

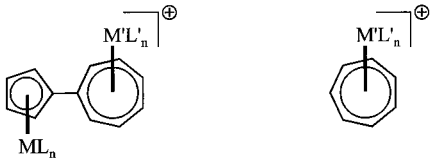

Figure 2. Archetype sesquifulvalene complexes of the general composition $[MLFe\{\mu\text{-}(\eta^5\text{-}C_5H_4)(\eta^7\text{-}C_7H_6)\}M'L']^+$ [ML = $(\eta^5\text{-}C_5H_5)Fe$; M′L′ = $Cr(CO)_3$ (**3**), none (**4**), $Ru(\eta^5\text{-}C_5H_5)^+$ (**5**), $Ru(\eta^5\text{-}C_5Me_5)^+$ (**6**)], and the tropylium cation **7** and its M′L′ complexes [M′L′ = none (**7**), $Cr(CO)_3$ (**8**), $Ru(\eta^5\text{-}C_5H_5)^+$ (**9**), $Ru(\eta^5\text{-}C_5Me_5)^+$ (**10**)]

Results and Discussion

Synthesis

For the cationic target complexes the starting compound is the monohydro-sesquifulvalene complex **1**, which is readily prepared by the nucleophilic addition of monolithiated ferrocene[8] to the tropylium cation (Scheme 1a).[3,4] The subsequent preparation of the cationic dipolar sesquifulvalene complexes is determined by the nature of the electron-accepting function. The reaction of the cycloheptatriene complex **1** with $Cr(CO)_3(EtCN)_3$ [9] yields the dimetallic monohydro-sesquifulvalene complex **2** (Scheme 1b) which is converted into the dipolar monocationic, dinuclear product **3** after the hydride elimination by the trityl cation (Scheme 1c).

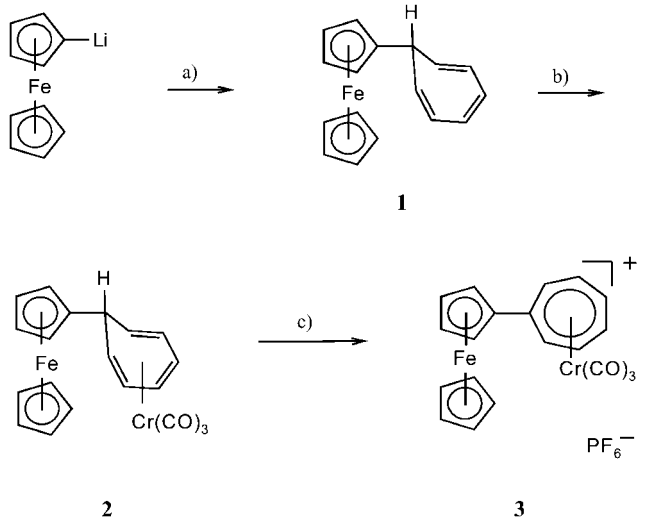

Scheme 1. Synthesis of the dimetallic monohydro-sesquifulvalene complexes **2** and the formation of the monocationic dinuclear sesquifulvalene complex **3:** a) $[C_7H_7]PF_6$, Et_2O; b) $Cr(CO)_3(EtCN)_3$, THF; c) $[Ph_3C]PF_6$, CH_2Cl_2

The preparation of the dicationic congeners **5** and **6** occurs by a hydride abstraction from **1**, revealing the cationic ferrocenyl-substituted tropylium compound **4**,[10] and is accomplished by the coordination of the proper metal−ligand fragment $Ru(\eta^5\text{-}C_5R_5)^+$ [11a,11b] to the tropylium moiety (Scheme 2).

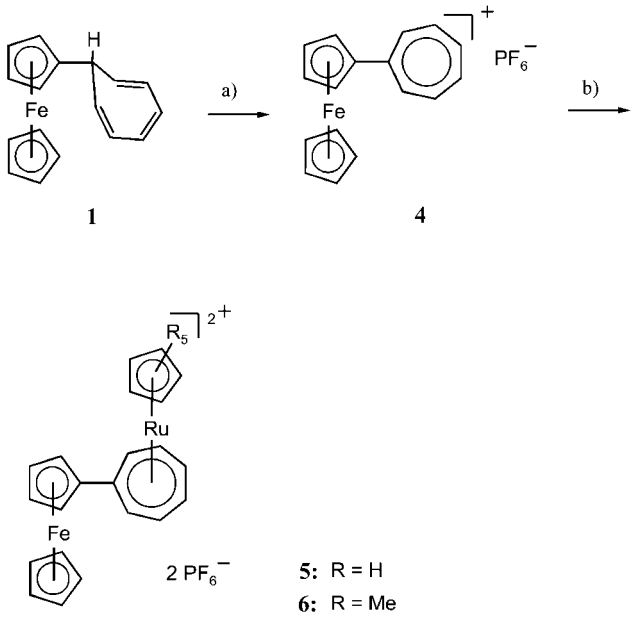

Scheme 2. Synthesis of the monometallic monocationic and dinuclear dicationic sesquifulvalene complexes **4**, **5**, and **6**, respectively: a) $[Ph_3C]PF_6$, CH_2Cl_2; b) $[(\eta^5\text{-}C_5R_5)Ru(MeCN)_3]PF_6$ (R = H, Me), CH_2Cl_2

Most remarkable in the course of the synthesis of the cationic sesquifulvalene complexes is a dramatic color change upon hydride abstraction. The dichloromethane solutions of the ferrocenyl derivatives change color from orange or brick-red to deep green-blue on going from the neutral monohydro-sesquifulvalene complexes to the cationic sesquifulvalene species.

NMR Spectroscopy

The assignment of the ^1H and ^{13}C NMR signals was performed using the splitting pattern in the ^1H NMR spectra, and by means of $^1H^1H$ and $^1H^{13}C$ correlation spectroscopy. From the NMR spectroscopic data in Table 1, which also includes the data of the unsubstituted tropylium cation and its M′L′ complexes [M′L′ = $Cr(CO)_3$ (**8**), $Ru(\eta^5\text{-}C_5H_5)^+$ (**9**), $Ru(\eta^5\text{-}C_5Me_5)^+$ (**10**)], it becomes evident that the shift ranges of the acceptor of the sesquifulvalene complexes correspond to the shifts of the signals of the unsubstituted tropylium cation **7** and its complexes **8**−**10**. In general a high-field shift of the signals of the tropylium moiety is also observed when the ferrocenyl donor is bound to the seven-membered ring. This effect of the donor substituent is also recognized for the distal ligands L′ whose signals are slightly high-field shifted when **5** and **6** are compared with **9** and **10**. Additionally, the small low-field shift of the resonance signal of the carbonyl ligands in **3** compared to **8** is in agreement with a slight increase in electron density on the metal center Cr, upon donor substitution on the tropylium ring. The high-field shift of the resonance signals of

Table 1. ^{1}H and ^{13}C NMR shifts of the cationic sesquifulvalene complexes $[(\eta^5\text{-}C_5H_5)Fe\{\mu\text{-}(\eta^5\text{-}C_5H_4)(\eta^7\text{-}C_7H_6)\}M'L']^+$ [M′L′ = $Cr(CO)_3$ (**3**), none (**4**), $Ru(\eta^5\text{-}C_5H_5)^+$ (**5**), $Ru(\eta^5\text{-}C_5Me_5)^+$ (**6**)], and, for comparison, the ^{1}H and ^{13}C NMR spectroscopic data of the tropylium cation $[C_7H_7]^+$ (**7**) and its complexes $[(\eta^7\text{-}C_7H_7)M'L']^+$ [M′L′ = $Cr(CO)_3$ (**8**), $Ru(\eta^5\text{-}C_5H_5)^+$ (**9**), $Ru(\eta^5\text{-}C_5Me_5)^+$ (**10**)]

	^{1}H NMR[a]						^{13}C NMR[a]						
M′L′	C_5H_4	CpFe	1-,6-H	2-,5-H	3-,4-H	L′	C_5H_4	CpFe	C-7	C-1,-6	C-2,-5	C-3,-4	L′
$Cr(CO)_3$ (**3**)	4.97, 5.12	4.28	6.45	6.75	6.55	–	81.3, 70.8, 76.0	72.9	133.1	99.8	105.6	104.7	223.9 (CO_3)
none (**4**)	5.45, 5.51	4.41		8.26−8.49		–	84.5, 73.4, 81.8	75.7	175.8	147.9	148.1	148.8	–
$Ru(\eta^5\text{-}C_5H_5)^+$ (**5**)	5.33, 5.47	4.37	7.27	7.34	7.60	6.11 ($\eta^5\text{-}C_5H_5$)	81.4, 72.2, 81.5	75.4	138.7	92.9	102.0	104.1	91.3 ($\eta^5\text{-}C_5H_5$)
$Ru(\eta^5\text{-}C_5Me_5)^+$ (**6**)	5.27, 5.34	4.36	7.09	7.10	7.35	1.98 ($\eta^5\text{-}C_5Me_5$)	77.6, 71.6, 79.6	74.1	133.8	97.8	104.2	105.3	109.9 ($\eta^5\text{-}C_5Me_5$) 10.4 ($\eta^5\text{-}C_5Me_5$)
none (**7**)	–	–		9.38 (C_7H_7)		–	–	–		156.6 (C_7H_7)			
$Cr(CO)_3$ (**8**)	–	–		6.67 ($\eta^7\text{-}C_7H_7$)		–	–	–		106.5 ($\eta^7\text{-}C_7H_7$)			221.7 (CO_3)
$Ru(\eta^5\text{-}C_5H_5)^+$ (**9**)	–	–		7.8 ($\eta^7\text{-}C_7H_7$)		6.37 ($\eta^5\text{-}C_5H_5$)	–	–		107.5 ($\eta^7\text{-}C_7H_7$)			93.1 ($\eta^5\text{-}C_5H_5$)
$Ru(\eta^5\text{-}C_5Me_5)^+$ (**10**)	–	–		7.48 ($\eta^7\text{-}C_7H_7$)		2.23 ($\eta^5\text{-}C_5Me_5$)	–	–		107.6 ($\eta^7\text{-}C_7H_7$)			112.6 ($\eta^5\text{-}C_5Me_5$) 10.9 ($\eta^5\text{-}C_5Me_5$)

[a] Solvent: CD_3NO_2 rel. TMS, numbering scheme see Figure 4.

the tropylium moiety goes along with a general low-field shift of the ferrocene signals, which increases in the order M′L′ = $Cr(CO)_3$ < $Ru(\eta^5\text{-}C_5Me_5)^+$ < $Ru(\eta^5\text{-}C_5H_5)^+$ < none. This behavior of the dipolar sesquifulvalene complexes **3**−**6** clearly elucidates a strong donor (metallocene)−acceptor (tropylium moiety) interaction in the ground state and, moreover, points to a growing charge delocalization in the same order.

Redox Properties

Cyclic voltammetry studies were conducted on all of the sesquifulvalene complexes as well as for the unsubstituted tropylium cation (**7**) and the corresponding mononuclear complexes $[(\eta^7\text{-}C_7H_7)M'L']^+$ [M′L′ = $Cr(CO)_3$ (**8**), $Ru(\eta^5\text{-}C_5H_5)^+$ (**9**), $Ru(\eta^5\text{-}C_5Me_5)^+$ (**10**)]. Electrochemical studies on **7**,[12] **8**,[13] and **9**[11a] have already been described. However, since the published data were obtained under different conditions, the reduction potentials of **7**−**9** were revised under conditions comparable to those applied for the sesquifulvalene complexes. As is known from the literature, the tropylium cation **7** and its complex congeners **8** and **9** undergo irreversible one-electron reduction steps, which is in agreement with the results obtained for the sesquifulvalene complexes (vide infra). The reduction potentials (Table 2) obtained for the tropylium derivatives **7**−**10** change in the order of M′L′ = $Cr(CO)_3$ < $Ru(\eta^5\text{-}C_5Me_5)^+$ < none < $Ru(\eta^5\text{-}C_5H_5)^+$, and illustrate an increase in the electron-withdrawing ability roughly in accordance with the NMR spectroscopic data.

Table 2. Cyclic voltammetry data of the cationic sesquifulvalene complexes $[(\eta^5\text{-}C_5H_5)Fe\{\mu\text{-}(\eta^5\text{-}C_5H_4)(\eta^7\text{-}C_7H_6)\}M'L']^+$ (**3**−**6**) and the mononuclear tropylium species $[(\eta^7\text{-}C_7H_7)M'L']^+$ (**7**−**10**)

M′L′		$E_{1/2}$ [a][b]	ΔE_p [c]	E_{pc} [a][b][d]	ΔE[e]
$Cr(CO)_3$	**3**	0.32	72	−1.14	1.46
none	**4**	0.42	74	−0.59	1.01
$Ru(\eta^5\text{-}C_5H_5)^+$	**5**	0.44	84	−0.61	1.05
$Ru(\eta^5\text{-}C_5Me_5)^+$	**6**	0.44	69	−0.84	1.28
none	**7**			−0.63[f][g]	
$Cr(CO)_3$	**8**			−1.20[h]	
$Ru(\eta^5\text{-}C_5H_5)^+$	**9**			−0.52[g]	
$Ru(\eta^5\text{-}C_5Me_5)^+$	**10**			−0.78	

[a] Obtained from $MeNO_2$ solutions, 0.4 M $[nBu_4N]PF_6$, room temperature, reference electrode Ag/AgCl. − [b] In V vs. $Fe(C_5H_5)_2/[Fe(C_5H_5)_2]^+$. − [c] $\Delta E_p = |E_{pa} - E_{pc}|$ in mV, ΔE_p(ferrocene) = 73 mV, scan rate: 100 mV/s. − [d] Peak potential of the irreversible one-electron reduction, scan rate: 100 mV/s. − [e] $\Delta E = E_{1/2} - E_{pc}$ in mV. − [f] See also ref.[12] − [g] See also ref.[11a] − [g] See also ref.[13]

The cyclic voltammograms of the corresponding cationic sesquifulvalene complexes **3**−**6** also reveal an irreversible one-electron reduction process in the potential domain of the unsubstituted tropylium species (Figure 3) in addition to an oxidation step in the range of free ferrocene. The potentials of the electrochemically irreversible reduction of the sesquifulvalene complexes are slightly cathodically shifted with respect to the unsubstituted tropylium cations **7**−**10** (Table 2) as expected, due to the electron-donating property of the ferrocenyl substituent.

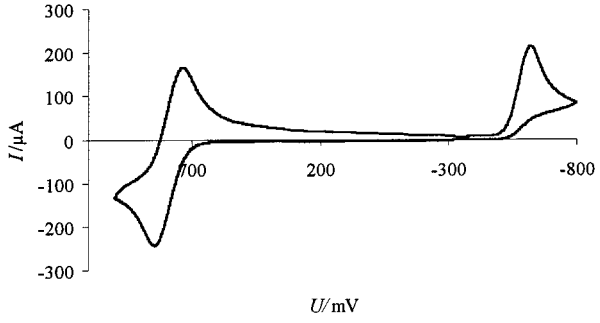

Figure 3. Representative cyclic voltammogram of the cationic sesquifulvalene complexes $[(\eta^5\text{-}C_5H_5)Fe\{\mu\text{-}(\eta^5\text{-}C_5H_4)(\eta^7\text{-}C_7H_6)\}M'L']^+$ [here M′L′ = none (**4**); for more details see Table 2]

The oxidation step involves an electrochemically reversible one-electron transfer, which is 320−440 mV anodically shifted with respect to free ferrocene (Table 2) caused by the electron-withdrawing ability of the tropylium moiety. The anodic shift of the oxidation potentials changes in the order M′L′ = $Cr(CO)_3$ < none < $Ru(\eta^5\text{-}C_5Me_5)^+$ = $Ru(\eta^5\text{-}C_5H_5)^+$. This order differs somewhat from the outcome of

the NMR spectroscopic study. This may be due to the fact, that in the NMR spectroscopic studies only the donor−acceptor interaction of the ground state is measured, whereas in cyclic voltammetry experiments the donor−acceptor interactions of the starting complex as well as of the oxidized (or reduced) product, including reorganization energies, will contribute to the oxidation (or reduction) potential.

Assuming that the oxidation potentials roughly correlate with the energy of the HOMO and the reduction potentials to the energy of the LUMO, the differences of the redox potentials E (Table 2) allow the tentative conclusion that the HOMO−LUMO gap for the sesquifulvalene complexes **3**−**6** should roughly decrease in the order M′L′ = $Cr(CO)_3$ > $Ru(\eta^5\text{-}C_5Me_5)^+$ > $Ru(\eta^5\text{-}C_5H_5)^+$ > none.

Crystal Structure Analyses

Crystal structure analyses were obtained for all of the sesquifulvalene complexes studied, and selected structural data are listed in Table 3. The crystal structure of complex **3** [M′L′ = $Cr(CO)_3$] has already been published,[3] as well as the molecular structure of **4** as a hexafluorophosphate salt.[14] However, **4** was synthesized as a tetrafluoroborate salt and the molecular structure data were obtained with higher accuracy.[4]

Solving the molecular structure of complex **6** [M′L′ = $Ru(\eta^5\text{-}C_5Me_5)^+$] proved to be more difficult because of the presence of three different independent molecules, and the intercalation of four independent solvent molecules of $MeNO_2$ as evidenced by means of NMR spectroscopy and elemental analysis. The structural data of all three independent molecules of **6** are in agreement within the margin of error. In Table 3 the selected structural data of only one independent molecule of the unit cell of **6** are presented. The molecular structures of the sesquifulvalene complexes **5** and **6** are depicted in Figure 4.

The molecular structures of the sesquifulvalene complexes **3**−**6** have an almost coplanar alignment of the sesquifulvalene rings. The twisting angle between the best planes of the five- and seven-membered rings varies between 0 and 17° for **4** and **6**, respectively. The dinuclear complexes exhibit a *transoid* conformation of the complex moieties due to the nonbonding repulsions between the metal fragments in a *cisoid* conformation. A *cisoid* conformation is observed only for complexes with increased length of the π-bridge between the five- and seven-membered ring.[3−7]

Since mutual electronic influence of the donor and acceptor group is expected to affect the molecular structure, the discussion concerning the structural details is focussed on geometric parameters directly related to the sesquifulvalene entity (Figure 5). As for sesquifulvalenes themselves the bonding situation in their complexes can in principle be described in terms of two mesomeric forms, the bis(aromatic) form **A** and the cross-conjugated form **B** (Figure 1), which is composed of an η^6-fulvene complex and a free or coordinated cycloheptatriene moiety. For both types of complexes characteristic structural features are expected

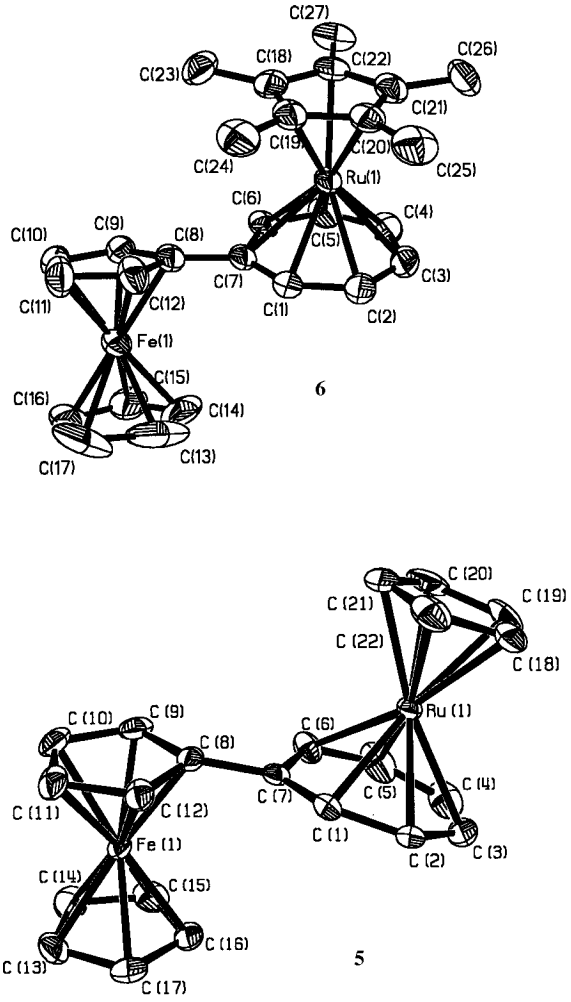

Figure 4. Molecular structures of the cationic sesquifulvalene complexes $[(\eta^5\text{-}C_5H_5)Fe\{\mu\text{-}(\eta^5\text{-}C_5H_4)(\eta^7\text{-}C_7H_6)\}M'L']^+$ [M′L′ = $Ru(\eta^5\text{-}C_5H_5)^+$ (**5**), $Ru(\eta^5\text{-}C_5Me_5)^+$ (**6**); 50% ellipsoids, the hydrogen atoms, solvent molecules and counter ions are omitted for clarity, for **6** only one independent molecule is shown]

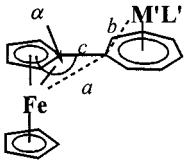

Figure 5. Schematic presentation of the molecular structure of the sesquifulvalene complexes including the notations of special geometric parameters found in Table 3

which are known from corresponding mononuclear complexes and their uncoordinated monocyclic organic species.[15−17]

In fact, a comparison of the structural data listed in Table 3, on average, reveals a characteristic long-short pattern of the endocyclic C−C bonds for the coordinated or free tropylium moiety, which is less significant in the dinuclear species. In accordance to it, the C−C distances between the bridge-head carbon atom C8 and the proximal carbon atoms C9 and C12 of the five-membered ring are distinctly longer than the C−C distances within the endocyclic buta-

Table 3. Selected interatomic distances [pm] and angles [°] (compare Figure 5) of the cationic sesquifulvalene complexes $[(\eta^5\text{-}C_5H_5)Fe\{\mu\text{-}(\eta^5\text{-}C_5H_4)(\eta^7\text{-}C_7H_6)\}M'L']^+$ [M′L′ = $Cr(CO)_3$ (**3**), none (**4**), $Ru(\eta^5\text{-}C_5H_5)^+$ (**5**), $Ru(\eta^5\text{-}C_5Me_5)^+$ (**6**)] and the corresponding structural parameters of the fulvene complex $[(\eta^5\text{-}C_5H_5)Fe\{\eta^6\text{-}C_5H_4C(C_6H_5)_2\}]BF_4$ (**11**) (see ref.[17a])

M′L′ =	$Cr(CO)_3$ [a] **3**	none[b] **4**	$Ru(\eta^5\text{-}C_5H_5)^+$ **5**	$Ru(\eta^5\text{-}C_5Me_5)^+$ **6**	**11**[c]
C1−C7	141.1(10)	141.5(3)	142.7(4)	143.1(7)	
C1−C2	137.7(12)	137.7(4)	140.4(4)	141.3(8)	
C2−C3	140.3(12)	140.0(4)	141.0(5)	142.7(9)	
C3−C4	138.5(14)	136.1(7)	137.7(6)	141.4(9)	
C4−C5	139.7(13)		141.8(6)	142.0(9)	
C5−C6	138.9(11)		140.8(4)	140.8(8)	
C6−C7	141.4(10)		142.7(4)	144.3(7)	
C7−C8[d]	145.1(10)	145.0(5)	145.2(4)	145.3(7)	141.6(10)
C8−C9	144.1(10)	144.6(3)	144.9(4)	144.7(7)	144.5(10)
C8−C12	143.7(10)		144.1(4)	144.6(8)	143.8(10)
C9−C10	141.2(12)	142.7(4)	141.4(5)	141.7(9)	140.2(11)
C10−C11	138.6(12)	141.2(6)	141.0(5)	142.1(10)	142.5(11)
C11−C12	138.4(12)		141.7(4)	142.3(9)	141.3(9)
Fe···C7[e]	305.0(7)	305.1(3)	290.4(4)	303.9(6)	271.5(6)
Fe−C8	202.0(6)	203.5(3)	201.3(3)	202.5(5)	200.9(7)
Fe−C9	202.0(7)	204.8(3)	202.7(3)	203.7(5)	201.8(8)
Fe−C10	203.1(9)	206.8(3)	206.3(3)	203.7(6)	208.5(8)
Fe−C11	206.0(8)		206.6(3)	205.0(7)	209.5(6)
Fe−C12	204.4(7)		203.9(3)	202.3(6)	206.0(8)
M′−Cn[f]	221.4(7)− 224.1(7)		226.0(6)− 228.2(5)	222.5(3)− 227.4(3)	
M′−C7[g]	232.0(6)		244.7(3)	234.2(5)	
α[h] [°]	176.5	175.5	167.5	174.7	159.3
γ[i] [°]	10.0(4)	0.0	10.5(4)	17.0(3)	

[a] Ref.[3] − [b] Ref.[4] − [c] Ref.[17a] − [d] Bridging carbon−carbon bond *c*. − [e] Nonbonding Fe−C7 distance *a*. − [f] Cn denotes C1−C6 of the tropylium moiety, only the upper and lower values are given. − [g] Metal−carbon bond *b*. − [h] Bending angle between the vector which bisects the substituted five-membered ring and includes the bridge-head carbon atom C8, and the vector of the carbon−carbon bond C7−C8. − [i] γ denotes the twisting angle between the five- and seven-membered ring.

diene unit C9...C12. A similar bond length variation is found in η^6-fulvene complexes, although to a larger extent.[17] This characteristic bond length pattern goes along with a decrease of the bending angle α and the distance *a* between the Fe atom of the ferrocenyl unit and the bridge-head carbon atom C7 of the seven-membered ring, which are the most important structural features indicating the contribution of the cross-conjugated mesomeric form **B** to the electronic ground state (see Figure 1). The bending angle α and the distance Fe···C7 decrease in the order M′L′ = $Cr(CO)_3$ > $Ru(\eta^5\text{-}C_5Me_5)^+$ > none > $Ru(\eta^5\text{-}C_5H_5)^+$. Similarly, a considerable increase of the bond length *b* between M′ (Cr or Ru) and C7 is observed with respect to the remaining metal−carbon bond lengths of the tropylium complexes (M′−Cn, see Table 3), which amounts to about 10 pm for **3** and **6**, but about 20 pm for **5**. Apparently, the gradual change from an aromatic to a fulvene-like coordination mode is a result of an increased D−A interaction due to the growing electron-withdrawing ability of the acceptor.[18]

Electronic Excitation

UV/Vis spectroscopic studies were performed with solutions of different solvent polarity such as dichloromethane and nitromethane, to elucidate solvatochromism which gives an indication of the dipole change Δμ between the ground and the excited state,[19] and is thus relevant for the first hyperpolarizability β according to the two-level approximation.[20,21] The UV/Vis spectra of the complexes under study contain two strong absorption bands in the visible and near-UV region (Figure 6, Table 4), which undergo considerable negative solvatochromism, i.e. hypsochromic shift with increasing solvent polarity. These two bands are characteristic for dipolar ferrocene bearing NLO chromophores. Recently, it was shown by means of DF calculations that for (*E*)-1-ferrocenyl-2-(*p*-nitrophenyl)ethene the high-energy absorption band must be assigned to a cyclo-

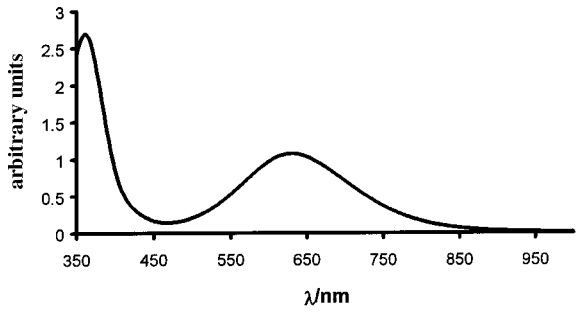

Figure 6. Representative UV/Vis spectrum of the dinuclear sesquifulvalene complexes $[(\eta^5\text{-}C_5H_5)Fe\{\mu\text{-}(\eta^5\text{-}C_5H_4)(\eta^7\text{-}C_7H_6)\}M'L'](PF_6)_2$ [here: M′L′ = $Ru(\eta^5\text{-}C_5H_5)$ (**5**)] obtained from CH_2Cl_2 solution

Table 4. UV/Vis data of the cationic sesquifulvalene complexes $[(\eta^5\text{-}C_5H_5)Fe\{\mu\text{-}(\eta^5\text{-}C_5H_4)(\eta^7\text{-}C_7H_6)\}M'L']^+$ [$M'L' = Cr(CO)_3$ (**3**), none (**4**), $Ru(\eta^5\text{-}C_5H_5)^+$ (**5**), $Ru(\eta^5\text{-}C_5Me_5)^+$ (**6**)], and the experimental first hyperpolarizability β obtained by means of hyper-Raleigh scattering measurements (see ref.[24])

	λ_{max}(LA−CT)[a][b] (ε)[c]			λ_{max}(DA−CT)[a][b] (ε)[c]				
M′L′	CH_2Cl_2	$MeNO_2$	$\Delta\tilde{\nu}$[d]	CH_2Cl_2	$MeNO_2$	$\Delta\tilde{\nu}$[d]	β[HRS][e] [f]	β_0[g] [f]
$Cr(CO)_3$ (**3**)	408 (2600)	395	−807	590 (3100)	574 (4880)	−473	n.d.[h]	
none (**4**)	400 (14710)	395 (13355)	−317	725 (3565)	700 (3335)	−493	f[i]	
$Ru(\eta^5\text{-}C_5H_5)^+$ (**5**)	374	–		637	614 (5270)	−588	125	28
$Ru(\eta^5\text{-}C_5Me_5)^+$ (**6**)	360	–		628	605 (4510)	−605	115	23

[a] Obtained from ca. 10^{-5} M solutions. – [b] λ_{max} in nm. – [c] Extinction coefficient in $M^{-1}cm^{-1}$. – [d] $\Delta\tilde{\nu} = \tilde{\nu}(CH_2Cl_2) - \tilde{\nu}(MeNO_2)$ in cm^{-1}. – [e] Referenced against *p*-nitroaniline (*p*-NA): $\beta(MeNO_2) = 34.6 \cdot 10^{-30}$ esu[37]. – [f] Given as units of 10^{-30} esu. – [g] Calculated from $\beta_0 = \beta(HRS)\,[(1-4\lambda^2_{max}/\lambda^2)(1-\lambda^2_{max}/\lambda^2)]$.[21] – [h] n.d.: HRS signal not detectable. – [i] f: fluorescent.

pentadienyl ligand−acceptor charge-transfer (L−A CT) transition whereas the low-energy absorption band is caused by a donor (metal)−acceptor charge-transfer (D−A CT) transition.[22] The CT transitions both provide a delocalization or even transfer of the positive charge from the tropylium moiety to the donor upon excitation, which is experimentally proven by the negative solvatochromism.[23]

This assignment is also supported by the fact that both of the CT transitions are strongly influenced by the nature of the acceptor, which is in accordance with recently published results about sesquifulvalene complexes with more extended π-bridges between the metallocene donor and the tropylium moiety acceptor.[3−5] However, the electronic influence of the acceptor on the L−A and D−A CT transitions is different. The D−A CT transitions decrease in energy in the order $M'L' = Cr(CO)_3 > Ru(\eta^5\text{-}C_5Me_5)^+ > Ru(\eta^5\text{-}C_5H_5)^+ >$ none. This order correlates with that of the HOMO−LUMO splitting assumed from the cyclic voltammetry results. The order varies for the L−A CT transition: $M'L' = Ru(\eta^5\text{-}C_5Me_5) > Ru(\eta^5\text{-}C_5H_5)^+ >$ none $> Cr(CO)_3$. The extraordinary low-energy shift of the D−A CT band of the mononuclear complex **4** compared to the dinuclear species may be explained by the formation of additional molecular orbitals (MO) upon coordination of a metal−ligand fragment, thus forming occupied bonding MOs which would be lower in energy, and empty antibonding MOs which would be higher in energy compared to the orbitals of the initial uncoordinated tropylium moiety.

As mentioned before the electronic excitations are governed by a distinct blue-shift on increasing the solvent polarity. The extent of the solvatochromism for both of the absorption bands can only be determined for **3** and **4**, since the maximum of the high-energy L−A CT absorption band of **5** and **6** in CH_3NO_2 is too far blue-shifted into the absorption region of the solvent to be determined. Nevertheless, from the obtained data it turns out that the change in polarity is similar for both of the CT transitions, and hence both should contribute to the first hyperpolarizability.[20,21]

NLO Measurements

The low-lying excited states of the sesquifulvalene complexes under study along with their facile polarizability, indicated by their pronounced solvatochromism, makes these types of complexes very promising for the second harmonic generation. Due to the cationic nature of the sesquifulvalene complexes the hyper-Rayleigh scattering (HRS)[24] is the only method for determining the first hyperpolarizability β which represents the molecular capability of transforming incoming light with frequency ω to frequency 2ω. However, a draw-back of the HRS method may be fluorescence due to two-photon absorption.[25−27] After realizing the problem of multiphoton absorption induced fluorescence concerning the determination of the first hyperpolarizability, several techniques have been investigated to overcome this problem. These include long-wavelength measurements,[28,29] time-resolved HRS[28] measurements of the two-photon fluorescence spectrum to abstract the fluorescence contribution to the HRS signal,[30] and a high-frequency demodulating technique to suppress the multiphoton fluorescence contribution to the HRS signal.[25]

A ''low-cost'' check for the two-photon fluorescence was recently described,[4,5] and uses bandpass filters with peak transmittance at different wavelengths introduced in front of the photomultiplier of the HRS set-up. The broad fluorescence signal, which yields the emission maximum at λ/2 of the fundamental wavelength, is easily discerned from the narrow second harmonic signal at λ/2.

In the course of this study the mononuclear complex **4** indicates two-photon fluorescence (Figure 7) whereas for **3** no intensity for the second harmonic signal was detected (Table 4). For the remaining complexes **5** and **6** the first hyperpolarizability β has been determined. The static first hyperpolarizability β_0 has been calculated by means of the two-level model,[21] taking into account the low-energy D−A CT transition. Nevertheless, it has to be emphasized that the high-energy L−A CT transition will also contrib-

ute to the first hyperpolarizability as indicated by the solvatochromism. The experimentally obtained first hyperpolarizability β and the calculated static hyperpolarizability β_0 for **5** and **6** (Table 4) are comparable although slightly larger for **5** with M′L′ = Ru(η^5-C_5H_5)$^+$ which has been shown to be the stronger electron-accepting moiety by means of NMR spectroscopy and cyclic voltammetry studies. However, the β and β_o values are not large and are comparable with the ferrocenyl-substituted (borabenzene)cobalt complex cation [CpFe{μ-(η^5-C_5H_4)(η^6-B(C_5H_5)}CoCp]$^+$.[18] Their values are difficult to discuss with respect to increasing D−A interaction due to (i) the margin of error in the determination of the first hyperpolarizability by HRS, (ii) the fact that the SHG signal occurs in the region of considerable D−A CT absorption, and (iii) the contribution of both the L−A CT and D−A CT transition to the SHG.

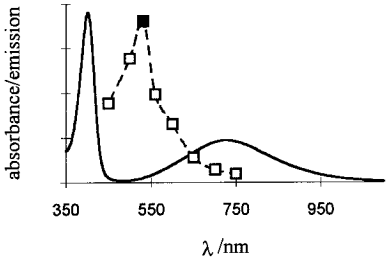

Figure 7. Absorption and emission spectrum of **4**

Conclusions

A series of cationic ferrocenyl-containing mono- and dimetallic dipolar sesquifulvalene complexes [CpFe{μ-(η^5-C_5H_4)(η^7-C_7H_6)M′L′]$^+$ [M′L′ = $Cr(CO)_3$, none, Ru(η^5-C_5H_5)$^+$, Ru(η^5-C_5Me_5)$^+$] were synthesized and both spectroscopically and structurally characterized. In these complexes the metallocenyl unit acts as an electron donor and the positively charged tropylium moiety as an electron acceptor. From the NMR spectroscopic data an increased delocalization of the positive charge is concluded for the ground state in the series M′L′ = $Cr(CO)_3$ < Ru(η^5-C_5Me_5)$^+$ < Ru(η^5-C_5H_5)$^+$ < none. The increased delocalization of the positive charge goes along with a growing contribution of the cross conjugated mesomeric form **B** to the bis(aromatic) mesomeric form **A** in the electronic ground state (Figure 1) as confirmed by gradual structural changes: i) the increasing bond length alternation in the five-membered ring, ii) the decreasing bending angle α between the C_5H_4 plane and the bonding vector of the bond C7−C8 linking the five- and seven-membered ring, and iii) the decreasing distance between the Fe atom of the ferrocene and the bridge-head carbon atom C7 of the seven-membered ring. The electronic excitation reveals two absorption bands in the visible and near-UV region that are assigned to an energetically low-lying D−A CT transition and an energetically higher lying L−A CT transition. Both CT transitions will contribute to the efficiency of the second harmonic generation. However, the first hyperpolarizability β, which is determined by HRS, is only obtained for the dinuclear species **5** [M′L′ = Ru(η^5-C_5H_5)$^+$] and **6** [M′L′ = Ru(η^5-C_5Me_5)$^+$]. For complex **4** fluorescence was observed whereas for **3** no SHG could be observed.

Experimental Section

Manipulations were carried out under dry nitrogen using standard Schlenk techniques. Solvents were saturated with nitrogen. Diethyl ether (Et_2O), tetrahydrofuran (THF), *n*-hexane and toluene were freshly distilled from the appropriate alkali metal or metal alloy. Dichloromethane (CH_2Cl_2) and nitromethane ($MeNO_2$) were dried with calcium hydride. NMR: Varian Gemini 200 BB; Bruker AM 360; measured at 295 K rel. TMS. UV/Vis: Perkin−Elmer Model 554. IR: nujol mull, KBr cells, FT-IR, Perkin−Elmer Model 325. MS: Finnigan MAT 311 A (EI-MS). Elemental analyses: CHN-O-Rapid, Fa. Heraeus. Tropylium hexafluorophosphate (**7**),[31] monolithioferrocene,[8] triphenylcarbenium hexafluorophosphate/tetrafluoroborate,[32] tricarbonyltris(propionitrile)chromium(0),[9,33] tris(acetonitrile)(η^5-cyclopentadienyl)ruthenium(II) hexafluorophosphate,[34] tris(acetonitrile)(η^5-pentamethylcyclopentadienyl)ruthenium(II) hexafluorophosphate,[11b] tricarbonyl(η^7-cycloheptatrienylium)chromium(0) hexafluorophosphate (**8**),[35] (2,4,6-cycloheptatrien-1-yl)ferrocene (**1**), tricarbonyl[η^6-1-(ferrocenyl)cycloheptatriene]chromium(0) (**2**)[3,4] and tricarbonyl[(η^7-1-(ferrocenyl)cycloheptatrienylium]chromium(0) hexafluorophosphate (**3**)[3] were synthesized according to literature procedures.

1-(Ferrocenyl)cycloheptatrienylium Tetrafluoroborate ($4BF_4$): A solution of $[Ph_3C]BF_4$ (610 mg, 1.85 mmol) in CH_2Cl_2 (20 mL) was added to a solution of **1** (510 mg, 1.85 mmol) in CH_2Cl_2 (20 mL) and stirred for 30 min at room temperature. The color of the solution turned from brick-red to deep green-blue. The product precipitates on addition of Et_2O. The crystalline material was filtered off and recrystallized by gas-phase diffusion of Et_2O into a concentrated solution of $\mathbf{4}BF_4$ in CH_2Cl_2. Yield: 410 mg (61%) of black-blue cubes. ^{1}H NMR (CD_3NO_2): δ = 8.49−8.26 (m, 6 H, C_7H_6), 5.51 (pt, *J* = 2.0 Hz, 2 H, C_5H_4), 5.45 (pt, *J* = 2.0 Hz, 2 H, C_5H_4), 4.41 (s, 5 H, C_5H_5). ^{13}C NMR (CD_3NO_2): δ = 175.8 (C-7), 148.8 (C-3,-4), 148.1 (C-2,-5), 147.9 (C-1,-6), 84.5 [$C_q(C_5H_4)$], 81.8 (C_5H_4), 75.7 (C_5H_5), 73.4 (C_5H_4). IR (KBr): $\tilde{\nu}$ = 3100, 3060, 1498, 1443, 1383, 1272, 1084 (ν_{B-F}), 1059, 1035 cm^{-1}. $C_{17}H_{15}BF_4Fe$ (362.0): calcd. C 56.41, H 4.18; found C 56.14, H 4.16.

{(Tricarbonyl)(η^7-cycloheptatrienylium-1-yl)chromium(0)}ferrocene Hexafluorophosphate ($3PF_6$): The synthesis performed was slightly modified according to the literature procedure.[3] Instead of $[Ph_3C]BF_4$ the PF_6 salt was used. The reaction was conducted at 0 °C. Quantities used: [η^5-C_5H_5)Fe{μ-(η^5-C_5H_4)(η^6-C_7H_7)}Cr(CO)$_3$] (**2**) (150 mg, 0.36 mmol) in CH_2Cl_2 (20 mL), $[Ph_3C]PF_6$ (140 mg, 0.36 mmol) in CH_2Cl_2 (10 mL). Yield: 120 mg (61%) of blue-black needles. ^{1}H NMR (CD_3NO_2): δ = 6.75 (m, 2 H, 2-,5-H), 6.55 (dd, *J* = 6.1, 2.9 Hz, 2 H, 3-,4-H), 6.45 (d, *J* = 9.5 Hz, 2 H, 1-,6-H), 5.12 (pt, *J* = 2.0 Hz, 2 H, C_5H_4), 4.97 (pt, *J* = 2.0 Hz, 2 H, C_5H_4), 4.28 (s, 5 H, C_5H_5). ^{13}C NMR (CD_3NO_2): δ = 223.87 (CO), 133.13 (C-7), 105.59 (C-2,5), 104.71 (C-3,-4), 99.76 (C-1,-6), 81.32 [$C_q(C_5H_4)$], 75.97 (C_5H_4), 72.88 (C_5H_5), 70.82 (C_5H_4). IR (KBr): $\tilde{\nu}$ = 3100, 2038 (ν_{CO}), 1996 (ν_{CO}), 1549, 1487, 1384, 1291, 838 (ν_{P-F}) cm^{-1}; (CH_3NO_2): $\tilde{\nu}$ = 2054 (ν_{CO}), 2014 (ν_{CO}) cm^{-1}. UV/Vis (CH_3NO_2): λ_{max} (ε) = 395 (5280), 574 (4880) nm (M^{-1}·cm^{-1}). $C_{20}H_{15}CrF_6FeO_3P$ (556.2): calcd.: C 43.19, H 2.72; found C 42.68, H 2.97.

Generel Procedure for the Preparation of the Dicationic Dinuclear Sesquifulvalene Complexes: A solution of the monocationic tropylium compound **4** in CH_2Cl_2 was treated with an equimolar amount of the appropriate (cyclopentadienyl)ruthenium salt and stirred overnight. The precipitated product was filtered off, washed with CH_2Cl_2, and recrystallized from $MeNO_2/Et_2O$.

(η^5-Cyclopentadienyl)[η^7-1-(ferrocenyl)cycloheptatrienylium]-ruthenium(II) Bis(hexafluorophosphate) [5(PF_6)$_2$]: Quantities used: [(η^5-C_5H_5)Fe(η^5-C_5H_4−C_7H_6)]PF_6 (**4**PF_6) (280 mg, 0.67 mmol), [(η^5-C_5H_5)Ru(CH_3CN)$_3$]PF_6 (290 mg, 0.67 mmol), CH_2Cl_2 (30 mL). Yield: 402 mg (82%) of deep blue, rhombic plates. ^{1}H NMR (CD_3NO_2): δ = 7.60 (dd, *J* = 5.4, 2.0 Hz, 2 H, 3-,4-H), 7.34 (m, 2 H, 2-,5-H), 7.27 (d, *J* = 9.8 Hz, 2 H, 1-,6-H), 6.11 (s, 5 H, C_5H_5'), 5.47 (pt, 2 H, C_5H_4), 5.33 (pt, 2 H, C_5H_4), 4.37 (s, 5 H, C_5H_5). ^{13}C NMR (CD_3NO_2): δ = 138.7 (C-7), 104.1 (C-3,-4), 102.0 (C-2,-5), 92.9 (C-1,-6), 91.3 (C_5H_5'), 81.5 (C_5H_4), 81.4 [$C_q(C_5H_4)$], 75.4 (C_5H_5), 72.2 (C_5H_4). IR (KBr): $\tilde{\nu}$ = 3126, 1548, 1498, 1474, 1420, 1301, 1266, 834 (ν_{P-F}) cm^{-1}. UV/Vis (CH_3NO_2): λ_{max} (ε) = 614 (5270) nm ($M^{-1}\cdot cm^{-1}$). $C_{22}H_{20}F_{12}FeP_2Ru$ (731.3): calcd. C 36.14, H 2.76; found C 35.80, H 2.76.

[η^7-1-(Ferrocenyl)cycloheptatrienylium](η^5-pentamethylcyclopentadienyl)ruthenium(II) Bis(hexafluorophosphate) [6(PF_6)$_2$]: Quantities used: [(η^5-C_5H_5)Fe(η^5-C_5H_4−C_7H_6)]PF_6 (**4**PF_6) (160 mg, 0.38 mmol), [(η^5-C_5Me_5)Ru(CH_3CN)$_3$]PF_6 (192 mg, 0.38 mmol), CH_2Cl_2 (20 mL). Yield: 213 mg (70%) of violet-blue rhombic plates. ^{1}H NMR (CD_3NO_2): δ = 7.35 (m, 2 H, 3-,4-H), 7.10 (m, 2 H, 2-,5-H), 7.09 (d, *J* = 7.3 Hz, 2 H, 1-,6-H), 5.34 (pt, 2 H, C_5H_4), 5.27 (pt, 2 H, C_5H_4), 4.36 (s, 5 H, C_5H_5), 1.98 (s, 15 H, C_5Me_5). ^{13}C NMR (CD_3NO_2): δ = 133.8 (C-7), 109.9 (C_5Me_5), 105.3 (C-3,-4), 104.2 (C-2,-5), 97.8 (C-1,-6), 79.6 (C_5H_4), 77.6 [$C_q(C_5H_4)$], 74.1 (C_5H_5), 71.6 (C_5H_4), 10.4 (C_5Me_5). IR (KBr): $\tilde{\nu}$= 3086, 2978, 1628, 1546, 1474, 1383, 1292, 1027, 837 (ν_{P-F}) cm^{-1}. UV/Vis (CH_3NO_2): λ_{max} (ε) = 605 (4510) nm ($M^{-1}\cdot cm^{-1}$). $C_{27}H_{30}F_{12}FeP_2Ru \times 4/3(CH_3NO_2) \times 1/3\ H_2O$ (888.77): calcd. C 38.24, H 3.93, N 2.10; found C 37.01, H 3.89, N 2.13.

Tricarbonyl(η^7-cycloheptatrienylium)chromium(0) Hexafluorophosphate (8PF_6): The synthesis was performed with a slight modification from the literature procedure.[35] To a solution of [(η^6-C_7H_8)Cr(CO)$_3$] (190 mg, 0.8 mmol) in CH_2Cl_2 (10 mL), a solution of [Ph_3C]PF_6 (320 mg, 0.8 mmol) in CH_2Cl_2 (10 mL), was added. The reaction mixture was stirred for 30 min at room temperature. The product was precipitated upon addition of Et_2O. The crystalline material was filtered off and recrystallized by gas-phase diffusion of Et_2O into a concentrated solution of **8**PF_6 in $MeNO_2$. Yield: 210 mg (70%) of red cubes. ^{1}H NMR (CD_3NO_2): δ = 6.67 (s, C_7H_7). ^{13}C NMR (CD_3NO_2): δ = 221.69 (CO), 106.51 (C_7H_7). IR (KBr): $\tilde{\nu}$ = 3092, 2067 (ν_{CO}), 2026 (ν_{CO}), 1455, 839 (ν_{P-F}) cm^{-1}; ($MeNO_2$): $\tilde{\nu}$ = 2069 (ν_{CO}), 2029 (ν_{CO}) cm^{-1}. UV/Vis (CH_3NO_2): λ_{max} (ε) = 400 (sh) (160) nm ($M^{-1}\cdot cm^{-1}$). $C_{10}H_7CrF_6O_3P$ (372.1): calcd. C 32.28, H 1.90; found C 32.06, H 2.12.

Table 5. Crystallographic data of [(η^5-C_5H_5)Fe(η^5-C_5H_4)(C_7H_6)]BF_4 (**4**BF_4), [(η^5-C_5H_5)Fe{μ-(η^5-C_5H_4)(η^7-C_7H_6)}Ru(η^5-C_5H_5)](PF_6)$_2$ [**5**(PF_6)$_2$], [(η^5-C_5H_5)Fe{μ-(η^5-C_5H_4)(η^7-C_7H_6)}Ru(η^5-C_5Me_5)](PF_6)$_2$ [**6**(PF_6)$_2$]

	4	5	6
Empirical formula	$C_{17}H_{15}BF_4Fe$	$C_{22}H_{20}F_{12}FeP_2Ru$	$C_{28.33}H_{34}F_{12}FeN_{1.33}O_{2.83}P_2Ru$
Formula mass	361.95	731.24	888.77
T [K]	173(2)	173(2)	173(2)
λ [pm]	71.073	71.073	71.073
Crystal system	orthorhombic	triclinic	triclinic
Space group	*Pnma*	$P\bar{1}$	$P\bar{1}$
a [pm]	2175(2)	942.6(2)	1749.2(4)
b [pm]	990.0(2)	1059.2(1)	1756.9(4)
c [pm]	688.1(3)	1235.2(2)	1767.0(4)
α [°]	90	75.908(1)	90.94(3)
β [°]	90	89.32	90.99(3)
γ [°]	90	82.381(1)	91.23(3)
V [10^6 pm^3]	1482.0(15)	1185.59(3)	5427.8(19)
Z	4	2	6
$\rho_{calcd.}$ [mg/m^3]	1.622	2.048	1.625
μ [mm^{-1}]	1.055	1.490	0.999
F (000)	736	720	2664
Crystal size [mm^3]	0.6 × 0.4 × 0.1	0.6 × 0.3 × 0.05	0.8 × 0.5 × 0.3
Scan range [°]	2.78−30.10	1.70−29.13	2.31−27.56
Index range	$-1 \le h \le 30$	$-12 \le h \le 12$	$0 \le h \le 22$
	$-13 \le k \le 1$	$-14 \le k \le 14$	$-22 \le k \le 22$
	$-1 \le l \le 9$	$-16 \le l \le 7$	$-23 \le l \le 23$
Reflections measured	2293	8200	26691
Reflections unique	1773	5834	25070
R_{int}	0.0175	0.0358	0.0740
Parameters	131	343	1353
Reflections $I > 4\ \sigma(I)$	2293	5834	20345
GoF[a]	1.061	0.971	1.058
$R1/wR^2$ [$I > 2(I)$][b]	0.0496/0.1280	0.0371/0.0854	0.0792/0.2199
$R1/wR^2$ (all data)[b]	0.0690/0.1172	0.0452/0.0884	0.0923/0.2350
Resd. min/max. [e/Å^3]	−0.647/0.549	−1.59/1.02	−1.952/1.858

[a] GoF (goodness of fit) = $[\Sigma w(F_o^2 - F_c^2)^2/(n-p)]^{1/2}$ (*n* = numbers of reflections, *p* = numbers of parameters). − [b] $R1 = \Sigma||F_o| - |F_c||/\Sigma|F_o|$; $wR2 = [\Sigma w(F_o^2 - F_c^2)^2/\{\Sigma w(F_o^2)^2\}]^{1/2}$.

(η^7-Cycloheptatrienylium)(η^5-cyclopentadienyl)ruthenium(II) Bis-(hexafluorophosphate) [9(PF_6)$_2$]: The synthesis was performed with a slight modification from the literature[11a] (see also the preparations of **5**PF_6 and **6**PF_6). Quantities used: [C_7H_7]PF_6 (**7**) (120 mg, 0.5 mmol), CH_2Cl_2 (20 mL), [(η^5-C_5H_5)Ru(CH_3CN)$_3$]PF_6 (220 mg, 0.5 mmol). Yield: 160 mg (80%) of a pale yellow solid. ^{1}H NMR (CD_3NO_2): δ = 7.80 (s, 7 H, C_7H_7), 6.37 (s, 5 H, C_5H_5). ^{13}C NMR (CD_3NO_2): δ = 107.51 (C_7H_7), 93.07 (C_5H_5). IR (KBr): $\tilde{\nu}$ = 3127, 3085, 2971, 1458, 1421, 832 (ν_{P-F}) cm^{-1}. $C_{12}H_{12}F_{12}P_2Ru$ (547.2): calcd. C 26.34, H 2.21; found C 26.30, H 2.55.

(η^7-Cycloheptatrienylium)(η^5-pentamethylcyclopentadienyl)-ruthenium(II) Bis(hexafluorophosphate) [10(PF_6)$_2$]: The synthesis was performed under identical conditions as for **9**(PF_6)$_2$. Quantities used: [C_7H_7]PF_6 (**7**) (100 mg, 0.4 mmol), CH_2Cl_2 (20 mL), [(η^5-C_5Me_5)Ru(CH_3CN)$_3$]PF_6 (200 mg, 0.4 mmol). Yield: 150 mg (80%) of pale yellow prisms. ^{1}H NMR (CD_3NO_2): δ = 7.48 (s, 7 H, C_7H_7), 2.23 (s, 15 H, C_5Me_5). ^{13}C NMR (CD_3NO_2): δ = 112.58 (C_5Me$_5$), 107.60 (C_7H_7), 10.91 (C_5Me_5). IR (KBr): $\tilde{\nu}$ = 3084, 2972, 1475, 1456, 1420, 1391, 1082, 1028, 832 (ν_{P-F}) cm^{-1}. $C_{17}H_{22}F_{12}P_2Ru$ (617.4): calcd. C 33.07, H 3.49; found C 32.82, H 3.55.

X-ray Structure Determination: Crystals of **4**BF_4, **5**(PF_6)$_2$, and **6**(PF_6)$_2$ suitable for an X-ray structure determination, were obtained by gas-phase diffusion of Et_2O into an $MeNO_2$ solution of the complex. The data were collected with four-circle diffractometers [**4**BF_4, and **6**(PF_6)$_2$: Hilger and Watts, Mo-K_α, λ = 0.71073 Å; **5**(PF_6)$_2$: Siemens aix, Mo-K_α, λ = 0.71073 Å]. The structures were solved by direct methods (SHELXS-86) and the refinements on F^2 were carried out by full-matrix least-squares techniques (SHELXL-93).[36] All non hydrogen atoms were refined with anisotropic thermal parameters. The hydrogen atoms were refined with a fixed isotropic thermal parameter related by a factor of 1.2 to the value of the equivalent isotropic parameter of their carrier atom. Weights were optimized in the final refinement cycles. In the structure of **6**, four independent molecules of CH_3NO_2 are present within the asymmetric unit. The position of an additional water molecule could be detected and was refined. An extinction coefficient correction of 0.0011 was applied. For more information see Table 5. Crystallographic data for the structures reported in this paper have been deposited at the Cambridge Crystallographic Data Centre as supplementary publication no. CCDC-142001 [**5**(PF_6)$_2$], and -42000 [**6**(PF_6)$_2$]. Copies of the data can be obtained free of charge on application to CCDC, 12 Union Road, Cambridge CB2 1EZ, UK [Fax: (internat.) + 44−1223/336−033; E-mail: deposit@ccdc.cam.ac.uk].

Cyclic Voltammetry: Measurements were performed in $MeNO_2$ with 0.4 M [N(nBu)$_4$]PF_6 as supporting electrolyte. An Amel 5000 system was used with a Pt wire as the working electrode and a Pt plate (0.6 cm^2) as the auxiliary electrode. The potentials were measured against Ag/Ag$^+$ and are referenced against $E_{1/2}$([Fe(C_5H_5)$_2$]/[Fe(C_5H_5)$_2$]$^+$) = 0 V.

Hyper-Rayleigh Scattering: Hyper-Rayleigh scattering measurements were performed with a pulsed Nd:YAG laser at a wavelength of λ = 1064 nm. For the experimental setup see ref.[24] Solutions of the complexes in $MeNO_2$ with concentrations in the range of 10^{-4} to 10^{-6} M were used with *p*-nitroaniline as a reference [β($MeNO_2$) = 34.6·10^{-30} esu].[37] Fluorescence checks were made by replacing the interference filter in front of the photomultiplier tube with filters that have transmittances at 400, 450, 500, 532, 560, 600, 650, and 700 nm.[4]

Acknowledgments

This work was supported by the Deutsche Forschungsgemeinschaft (DFG, HE 1309/3), by the European Community (COST D4/003/94, TMR FMRX-CT98−0166), and by the Fonds der Chemischen Industrie. We thank the DEGUSSA AG for a donation of $RuCl_3$ and Sartorius GmbH for a donation of microfilters.

[1] [1a] S. R. Marder, D. N. Beratan, L.-T. Cheng, *Science* **1991**, *252*, 103. [1b] S. R. Marder, G. B. Gorman, F. Meyers, J. W. Perry, G. Bourhill, J.-L. Brédas, B. M. Pierce, *Science* **1994**, *265*, 632. [1c] F. Meyers, S. R. Marder, B. M. Pierce, J.-L. Brédas, *J. Am. Chem. Soc.* **1994**, *116*, 10703. [1d] S. R. Marder, B. Kippelen, A. K.-Y. Jen, N. Peyghambarian, *Nature* **1997**, *388*, 845.

[2] J.-L. Brédas, *Adv. Mater.* **1995**, *7*, 263.

[3] U. Behrens, H. Brussaard, U. Hagenau, J. Heck, E. Hendrickx, J. Körnich, J. G. M. van der Linden, A. Persoons, A. L. Spek, N. Veldmann, B. Voss, H. Wong, *Chem. Eur. J.* **1996**, *2*, 98.

[4] H. Wong, T. Meyer-Friedrichsen, T. Farrell, C. Mecker, J. Heck, *Eur. J. Inorg. Chem.* **2000**, 631.

[5] J. Heck, S. Dabek. T. Meyer-Friedrichsen, H. Wong, *Coord. Chem. Rev.* **1999**, *190−192*, 1217.

[6] [6a] M. Tamm, T. Jentzsch, W. Werncke, *Organometallics* **1997**, *16*, 1418. [6b] M. Tamm, A. Gregorzewski, T. Steiner, T. Jentzsch, W. Werncke, *Organometallics* **1996**, *15*, 4984. [6c] M. Tamm, A. Grzegorzewski, T. Steiner, *Chem. Ber./Recueil* **1997**, *130*, 225.

[7] M. Tamm, T. Bannenberg, K. Baum, R. Fröhlich, T. Steiner, T. Meyer-Friedrichsen, J. Heck, *Eur. J. Inorg. Chem.* **2000**, 1161.

[8] F. Rebiere, O. Samuel, H. B. Kagan, *Tetrahedron Lett.* **1990**, *31*, 3121; U. T. Müller-Westerhoff, Z. Yuan, G. Ingram, *J. Organomet. Chem.* **1993**, *463*, 163; D. Guillaneux, H. B. Kagan, *J. Org. Chem.* **1995**, *60*, 2502.

[9] G. J. Kubas, *Inorg. Chem.* **1983**, *22*, 692.

[10] M. Cais, A. Eisenstadt, *J. Am. Chem. Soc.* **1967**, *89*, 5468.

[11] [11a] R = H: A. M. NcNair, D. C. Boyd, D. A. Bohling, T. P. Gill, K. R. Mann, *Inorg. Chem.* **1987**, *26*, 1182. [11b] R = Me: B. Steinmetz, W. A. Schenk, *Organometallics* **1999**, *18*, 943; P. J. Fagan, M. D. Ward, J. C. Calabrese, *J. Am. Chem. Soc.* **1989**, *111*, 1698.

[12] A. M. Romanin, A. Venzo, A. Ceccon, *J. Electroanal. Chem.* **1980**, *112*, 147.

[13] A. M. Romanin, A. Ceccon, A. Venzo, *J. Electroanal. Chem.* **1981**, *130*, 245.

[14] S. K. Brownstein, E. J. Gabe, R. C. Hynes, *Can. J. Chem.* **1992**, *70*, 1011.

[15] M. J. Barrow, O. S. Mills, *J. Chem. Soc., Chem. Commun.* **1971**, 119.

[16] J. D. Dunitz, P. Pauling, *Helv. Chim. Acta* **1960**, *43*, 2188.

[17] [17a] U. Behrens, *J. Organomet. Chem.* **1979**, *182*, 89. [17b] M. Watanabe; I. Motoyama, T. Takayama, *J. Organomet. Chem.* **1996**, *524*, 9. [17c] S. Barlow, L. M. Henling, M. W. Day, S. R. Marder, *Chem. Commun.* **1999**, 1567. [17d] A. I. Yanovsky, Y. T. Struchkov, A. Z. Kreindlin, M. I. Rybinskaya, *J. Organomet. Chem.* **1989**, *369*, 125.

[18] U. Hagenau, J. Heck, E. Hendrickx, A. Persoons, T. Schuld, H. Wong, *Inorg. Chem.* **1996**, *35*, 7863.

[19] P. Suppan, N. Ghoneim, in: *Solvatochromism*, Paston Press, Ltd., Norfolk, **1997**; N. Mataga, T. Kubota, *Molecular Interactions and Electronic Spectra*; Marcel Dekker; New York, **1970**, chapter 8.

[20] L. Oudar, D. S. Chemla, *Chem. Phys.* **1977**, *66*, 2664.

[21] E. Hendrickx, K. Clays, A. Persoons, C. Dehu, J. L. Brédas, *J. Am. Chem. Soc.* **1995**, *117*, 3547.

[22] [22a] S. Barlow, H. E. Bunting, C. Ringham, J. C. Green, G. U. Bublitz, S. G. Boxer, J. W. Perry, S. R. Marder, *J. Am. Chem. Soc.* **1999**, *121*, 3715. [22b] S. Barlow, S. R. Marder, *Chem. Commun.* **2000**, 1555.

[23] C. Reichard, *Solvents and Solvent Effects in Organometallic Chemistry*, 2nd ed., VCH, Weinheim, **1988**.
[24] K. Clays, A. Persoons, *Rev. Sci. Instrum.* **1992**, *63*, 3285.
[25] K. Clays, E. Hendrickx, T. Verbiest, A. Persoons, *Adv. Mater.* **1998**, *10*, 643; G. Olbrechts, T. Munters, K. Clays, A. Persoons, O.-K. Kim, L.-S. Choi, *Opt. Mater.* **1999**, *12*, 221.
[26] J. J. Wolff, R. Wortmann, *Adv. Phys. Org. Chem.* **1999**, *32*.121.
[27] S. Stadler, G. Bourhill, C. Bräuchle, *J. Phys. Chem.* **1996**, *100*, 6927.
[28] S. Stadler, R. Dietrich, G. Bourhill, C. Bräuchle, *Opt. Lett.* **1996**, *21*, 251−253
[29] M. A. Pauley, C. H. Wang, *Rev. Sci. Instrum.* **1999**, *70*, 1277.
[30] N. W. Song, T.-I. Kang, S. C. Jeung, S.-J. Joan, B. R. Cho, D. Kim, *Chem. Phys. Lett.* **1996**, *261*, 307; O. K. Song, J. N. Woodford, C. H. Wang, *J. Phys. Chem. A* **1997**, *101*, 3222
[31] K. Conrow, *Org. Synth., Coll. Vol.* **1973**, vol. V, p. 1138.
[32] G. A. Olah, J. J. Svoboda, J. A. Olah, *Synthesis* **1972**, 544.
[33] J. A. S. Howell, B. F. G. Johnson, J. Lewis, *J. Chem. Soc., Dalton Trans.* **1974**, 293.
[34] T. P. Gill, K. R. Mann, *Organometallics* **1982**, *1*, 485.
[35] E. W. Abel, M. A. Bennett, R. Burton, G. Wilkonson, *J. Chem. Soc.* **1958**, 4559.
[36] G. M. Sheldrick, *SHELXS-86 − program for crystal structure determination*, University of Göttingen, Germany, **1986**; G. M. Sheldrick, *SHELXL-93 − program for crystal structure refinement*, University of Göttingen, Germany, **1993**.
[37] T. Verbiest, K. Clays, S. Samyn, J. Wolff, D. Reinhoudt, A. Persoons, *J. Am. Chem. Soc.* **1994**, *116*, 9320.

Received June 21, 2001
[I01222]